POLISH MARITIME RESEARCH Special Issue 2017 S3 (95) 2017 Vol. 24; pp. 49-57
10.1515/pomr-2017-0104

NONLINEAR PTO EFFECT ON PERFORMANCE OF VERTICAL AXISYMMETRIC WAVE ENERGY CONVERTER USING SEMI-ANALYTICAL METHOD

Ming Liu[1]
Hengxu Liu[2*]
Xiongbo Zheng[3]
Hailong Chen[2]
Liquan Wang[1]
Liang Zhang[2]
[1] College of Mechanical and Electrical Engineering, Harbin Engineering University, China
[2] College of Shipbuilding Engineering, Harbin Engineering University, China
[3] Collge of Science, Harbin Engineering University, China
* corresponding author

ABSTRACT

The wave energy, as a clean and non-pollution renewable energy sources, has become a hot research topic at home and abroad and is likely to become a new industry in the future. In this article, to effectively extract and maximize the energy from ocean waves, a vertical axisymmetric wave energy converter (WEC) was presented according to investigating of the advantages and disadvantages of the current WEC. The linear and quadratic equations in frequency-domain for the reactive controlled single-point converter property under regular waves condition are proposed for an efficient power take-off (PTO). A method of damping coefficients, theoretical added mass and exciting force are calculated with the analytical method which is in use of the series expansion of eigen functions. The loads of optimal reactive and resistive, the amplitudes of corresponding oscillation, and the width ratios of energy capture are determined approximately and discussed in numerical results.

Keywords: Wave energy converter (WEC); power take-off (PTO); capture width ratios; analytical method; eigen function

INTRODUCTION

With the oil and other fossil energy depletion and climate changing resulting from the greenhouse gas emission, low carbon, energy conservation and sustainable use, the renewable energy sources development and utilization are the most attractive themes of the world's energy development. Ocean energy is stored in the water in the inexhaustible renewable energy, including wave energy, tidal energy, tidal energy, thermal energy, salt and so on. The wave energy, which contains the kinetic energy and potential energy due to ocean surface wave can be considered to be of high value in the form of ocean energy and likely to become a new industry in the future. Using of the periodic wave motion characteristics, WEC converts the wave energy into mechanical energy or hydraulic energy, and then transforms it into the available energy. Many devices of WEC have been created and motivated a wide variety of investigations. We especially pay close attention to a representative type of WECs, called oscillating buoy, which has small dimensions comparing with the incoming wave length. At present, research on the oscillating buoy WEC is still mainly concentrated in Europe and other countries.

The most common buoy oscillating WEC is the use of its heave motion. Early work can be traced to 1984 in Japan Tanaka[1] (1984) developed a G-1T WEC which includes

a wedge floating buoy and sliding rail of breakwater. This is a typical WEC which is mainly based on heaving motion. The size of oscillating buoy at the waterline surface is 1.8(m) ×1.2(m) and oscillating buoy slide along the breakwater under wave action. Sea trial was carried out in Tokyo Bay and in order to deal with the continuous wave of output energy, the use of the hydraulic cylinder type of pneumatic accumulator to deal with the purpose of achieving stable energy. The corresponding period, Budal *et al.*[2] (1982) developed a kind of oscillating buoy WEC based on the principle of float, called Norwegian Buoy (Fig.1). The device is made of upright post which is connected to the bottom of the sea and spherical oscillating buoy which absorb wave energy through heaving motion along the upright post. In 1983, the device model with the diameter of 1(m) spherical oscillating buoy was carried out by sea trial in the Trondheim fjord. The device comprises a power output device, a wind impeller is installed in the inner of the device, and the power output can be adjusted effectively. Early research provides technical basis for further research and many kinds of heaving WEC generation have been developed in recent years. Representative work is that Prado[3] (2008) in Holland developed a kind of WEC called Archimedes Wave Swing (Fig.2). The supporter of device is fixed in the seabed. The floating buoy and the supporter are connected by a linear motor. Floating buoy generate electricity through its heaving motion in wave peak and valley. After theoretical calculation, a comprehensive sea trial test was carried out in 2001 and 2002. The sea trial test is very not ideal well since the device is submerged in the water and not very well seal installation. In 2004, they improved the installation program, using a new sealing method on the power output device and finally the sea tries to succeed. Soon later, Elwood *et al.*[4] (2009) research a L-10 WEC (Fig.3). The WEC is consisting of a deep draft cylinder and an annular floating buoy. Deep draft cylinder connected with seabed by tension type mooring and annular floating buoy on the wave slide along a track in cylinder. This design limits the movement of other degrees of freedom in addition to the vertical swing. They developed a prototype of the 10kW power plant, the middle cylindrical draft 6.7(m), float outer radius 3.5(m) and sea trials conducted in the Gulf of Oregon, Newport.

Fig. 1. Norwegian Buoy

Fig. 2. Archimedes Wave Swing

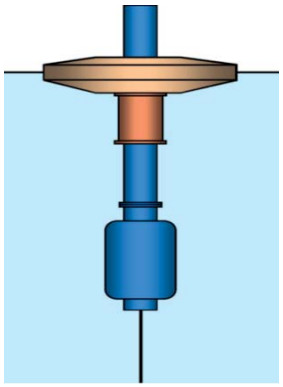

Fig 3. L-10

Another common buoy oscillating WEC is the use of its surging motion. It is well known that the wave force decreases with the increase of water depth. For this kind of WEC, the force along a shaft of a moving absorbing is usually converted to a moment of force. If that, surging motion converted to the pitching motion. So we usually called this type of WEC as flap WEC. According to the different installation position of the hinge shaft, flap WEC can be divided into two kinds of buoyant flap and suspension flap. Countries around the world have a lot of investment for the concept design and experimental research and practical applications of flap WEC and a number of typical flap WEC have been developed in recent years. Following are some brief introduction to the design and application of these classics. Cameron *et al.*[5] (2010) presented a flap WEC which consist of buoyancy flap, hydraulic cylinder, high pressure pipe and power station, called Oyster (Fig.4). The force pushes the buoyancy flap moving. The hydraulic cylinder, which is connected between the swing plate and the base, is compressed to convey the high pressure water to the shore through the submarine pipeline. A hydraulic motor is installed in the power station on the shore and high pressure water drive hydraulic motor and the hydraulic motor drives the generator to generate electricity. Currently Oyster has developed two generations of products. Different with flap WEC above, Finland AW-Energy company[6] (2010) developed a kind of flap WEC for generating electricity by using wave motion at sea floor,

called WaveRoller near shore ocean wave generator (Fig.5). It is installed on a platform at the bottom of the sea. Under the impetus of the waves, the blade of the WaveRoller generating set generates energy by swinging back and forth. After the hydraulic system is collected, the hydraulic motor and the generator are converted to electric energy by the shore. In 2003, WaveRoller generator for the first time at the Gulf of Finland small prototype pilot test. Soon Flocard and Finnigan [7] (2009) developed a flap WEC named BioWAVE (Fig.6). The base of the BioWAVE is fixed to the seabed and the flap buoy is hinged connect with the base. The flap buoy swings with the motion of the waves and in order to cope with the wave direction, the flap buoy can rotate around the vertical axis of the center of the base.

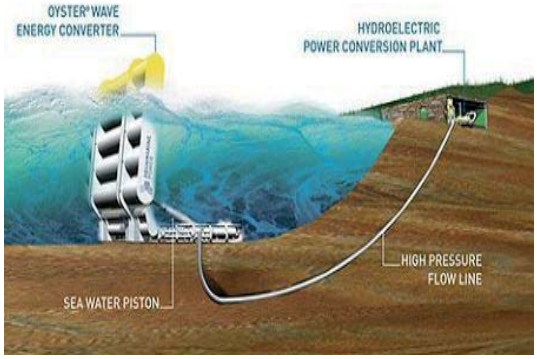

Fig. 4. Oyster

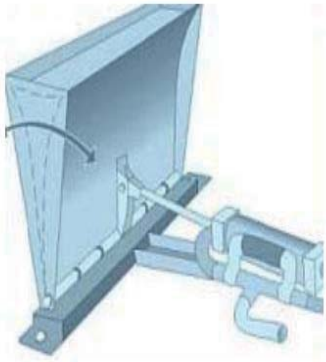

Fig. 5. WaveRoller

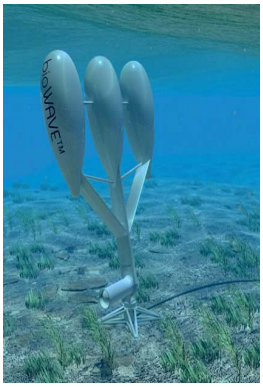

Fig. 6. BioWave

With several typical buoy oscillating WEC presented, scientists around the world began to research the theory of the concept model of buoy oscillating WEC, especially for its hydrodynamic characteristics and capture width ratios. For example, Mavrakos *et al.* [8] (2009) introduced into the traditional conical or cylindrical absorbers several creative structures, such as exterior torus, two piston-like arranged internal floater, and bottom-mounted vertical and horizontal skirts. And they analyzed the floaters geometries' effects of the wave energy converters, which is tightly moored, vertical and axisymmetric. These absorbers were comparatively evaluated in his research. Nazari *et al.*[9] (2013) analyzed and designed a point absorber of wave energy convertor for the wave condition of Assaluyeh coastal on Persian Gulf. In this analysis, he got the optimum wave power production by changing the shape of flat buoy to conical cylindrical to adjust the damping and natural frequency. Soulard[10] (2009) conducted the research works to create models and optimize the geometric of a two-body oscillating system, in which, a floating body forces against a submerged body through a linear power takeoff system and force reacting principle can be used. Goggins *et al.*[11] (2014) further developed this model by changing the geometry of floating oscillating absorber, optimized its hydrodynamic performance, and studied an unstrained WEC system. The offshore engineering groups, such as Chakrabarti *et al.*[12] (1983), Eatock Taylor *et al.* [13], (1983); Ran and Kim[14] (1995), studied vertical cylinders pivoted at the sea floor to articulated tower platform. Very recently, Caska and Finnigan[15] (2008) studied methods of hydrodynamic analysis for the application of a damped vertically oriented cylinder pivoted near the sea floor in the middle depth. Soon after, Stansby *et al.*[16] (2015) developed a wave energy absorber with a damped vertical bottom-pivoted cylinder and studied its motion response and corresponding power conversion capability.

The theory of the effect of the linear PTO comprising a linear spring and a linear damper was first presented by Evans[17] (1976) by a single freedom oscillating body under the regular waves. The linear PTO theory appeared subsequently in many other articals, and extened to multiple degree of freedom, such as Falnes (2002). Eriksson *et al.* [18] (2005) investigated the coupling response of the floating buoy and the linear generator under the frequency domain. Fitzgerald *et al.*[19] (2008) investigated the heave, surge and pitch motions of a moored WEC driven by regular waves, and also including results for the unmoored system with a linear PTO system. Price *et al.* [20] (2009) studied the WECs capture width detailedly, and discussed its influences of the linear PTO control.

Very recently, another important aspect of this research is truing to the quadratic PTO, such as Sheng and Lewis (2016). The problem becomes more complicated and much less research work have been done. The aim of this paper is to research quadratic PTO according to some claims have been made that quadratic PTO is better that the linear PTO due to quadratic PTO can convert more power than those of linear PTO. Thus in this work, the equation of linear and quadratic

PTO damping were carried out under the assumption of the linear hydrodynamics of a vertical axisymmetric WEC in regular waves. A method of damping coefficients, theoretical added mass and exciting force are calculated on the analytical method which is based on the series expansion of eigen functions. Numerical results concerning for optimizing resistive and damping PTO are presented to maximize wave energy.

MATHEMATICAL MODEL

The Sketch of the vertical axisymmetric WEC and the fluid divisions are shown in Fig.7. We defined a cylindrical coordinal system (r,θ,z), with the origin point o locating at the absorber center and in the plane of the mean free surface, and the axis oz being vertically upwards. The wetted surface of absorber is supposed to be consist of a cylindrical surface and a curved surface with vertical axisymmetry. The fluid domain due to the device can be divided into several sub-domain in order to obtain hydrodynamic coefficients.

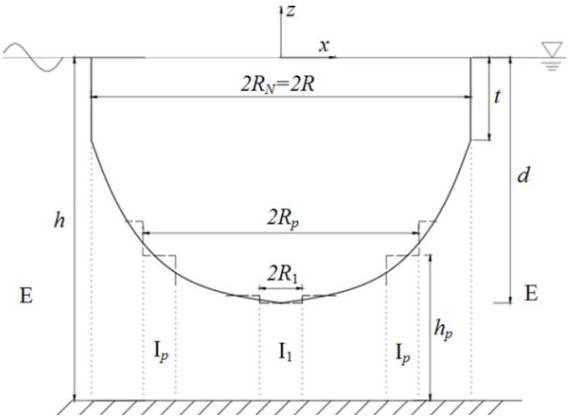

Fig. 7. The sketch of the device and the subdomain division

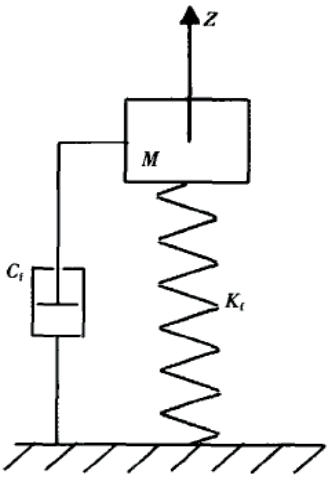

Fig. 8. Schematic diagram of wave energy conversion

WAVE ENERGY CONVERSION

The schematic diagram of wave energy conversion is shown in Fig.8. When a PTO is applied to connect the buoy and the fixed reference system such as seabed, the motion of the buoy can drive the PTO to convert the mechanical power into useful energy. Straightforward application of Newton's second law, the equation of motion in regular waves for the system is

$$M\ddot{X} = F_d + F_r + F_s + F_m \tag{1}$$

where M is the buoy mass; X is the displacement; the symbol F_d, F_r, F_s and F_m denote the wave excitation force, radiation force, hydrostatic restoring force and PTO force, respectively. Under the assumption of linear wave theory, the radiation and hydrostatic restoring force can be written as

$$\begin{aligned} F_r &= \mu\ddot{X} + \lambda\dot{X} \\ F_s &= bX \end{aligned} \tag{2}$$

Where μ stands for added mass; λ stands for damping coefficient; b is hydrostatic recovery coefficient. The PTO force can be separated two parts

$$F_m = F_m^k + F_m^c \tag{3}$$

And

$$\begin{aligned} F_m^k &= kX \\ F_m^c &= cf(\dot{X}) \end{aligned} \tag{4}$$

in which k is the stiffness coefficient of PTO; c is the damping coefficients of the PTO. For a linear PTO, the function of motion velocity in the pure damper is

$$f(\dot{X}) = \dot{X} \tag{5}$$

For a quadratic PTO, the function of motion velocity in the pure damper is

$$f(\dot{X}) = \dot{X}\left|\dot{X}\right| \tag{6}$$

Once the equation of motion is solved, the power conversion is simply calculated as

$$P = \left|F_m^c \dot{X}\right| \tag{7}$$

the corresponding average power is given by

$$\overline{P} = \frac{1}{T}\int_0^T P\mathrm{d}t \tag{8}$$

Where T is the time interval for calculating the average power.

HYDRODYNAMIC ANALYSIS

Hydrodynamic analysis of wave energy conversion is studied using a semi-analytical method is based upon eigen-function matching. For the linear wave theory, it is convenient to decompose the spatial velocity potential Φ as the follwoing part

$$\Phi = \Phi_0 + \Phi_7 + \sum_{j=1}^{6} \Phi_j \tag{9}$$

where Φ_0, Φ_7 stand for incident wave and diffraction velocity potential respectively. Φ_j (j=1...6) stand for radiated velocity potential for different motion modes. According to the potential flow theory, the aforementioned velocity potential should satisfied the following boundary condition,

Laplace boundary condition:

$$\nabla^2 \Phi_j = 0 \quad (j = 1,2\cdots 7) \quad \text{(in fluid domain)} \tag{10}$$

Freesurface boundary condition:

$$-f^2 \Phi_j + \partial_z \Phi_j = 0 \quad (j = 1,2\cdots 7) \quad (z = 0) \tag{11}$$

Bottom boundary condition:

$$\partial_z \Phi_j = 0 \quad (j = 1,2\cdots 7) \quad (z = -h) \tag{12}$$

Hull boundary condition:

$$\partial_n \Phi_j = V_n \quad (j = 1,2\cdots 6), \quad \partial_n \Phi_7 = -\partial_n \Phi_0 \tag{13}$$

Radiation boundary condition:

$$\lim_{r\to\infty} \sqrt{r}(\partial_r \Phi_j - ik_0 \Phi_j) = 0 \quad (j = 1,2\cdots 7) \tag{14}$$

in which $f^2 = \omega^2/g$, and ω is the wave frequency, g is the acceleration due to gravity. The wave number k_0 can be defined by the dispersion equation $k_0 \tanh k_0 h = f^2$, which is obtained by meeting the boundary condition. The V_n is the cylinder's velocity in the direction normal to the hull. The incident wave velocity potential in cylindrical coordinates (r,θ,z) can be given as

$$\Phi_0 = -\frac{Ag}{\omega} \sum_{\ell=0}^{\infty} \varphi_0^{\ell} \cos \ell\theta \tag{15}$$

With

$$\varphi_0^{\ell} = \varepsilon_{\ell} Z_0(z) \mathbf{J}_{\ell}(k_0 r) \tag{16}$$

where $\mathbf{J}_{\ell}(\cdot)$ is the first category Bessel function with the order ℓ and the expression for known function $Z_0(z)$ and coefficients ε_{ℓ} are given in the **Appendix A**. In the same way of incoming wave, diffraction velocity potential Φ_7 can be expressed as

$$\Phi_7 = -\frac{Ag}{\omega} \sum_{\ell=0}^{\infty} \varphi_7^{\ell} \cos \ell\theta \tag{17}$$

The potential of the radiation velocity, which is caused by the forced vertical axisymmetric body motion can be expressed as

$$\Phi_1 = \varphi_1^1 \cos\theta \tag{18}$$

in surge direction;

$$\Phi_3 = \varphi_3^0 \tag{19}$$

in heave direction;

$$\Phi_5 = \varphi_5^1 \cos\theta \tag{20}$$

in pitch direction.

To develop the velocity potentials of diffraction and radiation, the fluid domain can be developed into outer cylindrical sub-domain named as E and inner cylindrical sub-domains named as I_p ($1 \le p \le N$) as shown in Fig. 1. Velocity potential in domain E is

$$\varphi_j^{\ell,E} = \alpha_j^{\ell,E,0} Z_0(z) \frac{\mathbf{H}_{\ell}(k_0 r)}{\mathbf{H}_{\ell}^{'}(k_0 R)} + \sum_{n=1}^{\infty} \alpha_j^{\ell,E,n} Z_n(z) \frac{\mathbf{K}_{\ell}(k_n r)}{\mathbf{K}_{\ell}^{'}(k_n R)} + \Omega_j^{\ell,E}(r,z) \tag{21}$$

Where the $\mathbf{H}_{\ell}(\cdot)$ and $\mathbf{K}_{\ell}(\cdot)$ are the first category Hankel function and the modified second category Bessel function with the order ℓ separately. The wave number k_n is defined by dispersion equation $k_n \tan k_n h = -f^2$ for ($n \ge 1$). Velocity potential in domain I_1 is

$$\varphi_j^{\ell,I_1} = \alpha_j^{\ell,I_1,0} r^{\ell} + \sum_{n=1}^{\infty} \alpha_j^{\ell,I_1,n} \mathbf{I}_{\ell}(\lambda_n r) \cos \lambda_n (z+h) + \Omega_j^{\ell,I_1}(r,z) \tag{22}$$

In which, $\mathbf{I}_{\ell}(\cdot)$ is the second category Bessel function with the order ℓ. Velocity potential in domain I_p ($2 \le p \le N$) is

$$\begin{aligned} \varphi_j^{\ell,I_p} &= \alpha_j^{\ell,I_p,0} Q^{\ell,0}(r) + \sum_{n=1}^{\infty} \alpha_j^{\ell,I_p,n} Q^{\ell,n}(r) \cos \lambda_n (z+h) + \\ &+ \tilde{\alpha}_j^{\ell,I_p,0} \tilde{Q}^{\ell,0}(r) + \sum_{n=1}^{\infty} \tilde{\alpha}_j^{\ell,I_p,n} \tilde{Q}^{\ell,n}(r) \cos \lambda_n (z+h) + \Omega_j^{\ell,I_p}(r,z) \end{aligned} \tag{23}$$

In the velocity potentials' eigenfunction expansion, expressions for known function $Q(\cdot)$, $Z(\cdot)$ and $\Omega(\cdot)$ are listed in the **Appendix A** to make it easy for readers. The unknown coefficients α could be determined by Garrett's method[21-26], according to matching the potential and its normal derivative on the surface of concatenate boundaries, which is shared by the subdomains.

Once velocity potentials in six degree of freedom are known, hydrodynamic coefficients and diffraction wave forces of the absorber can be calculated by the integration of the pressure on the hull. In this research, single heave direction have been considered due to application in wave energy conversion. Thus, diffraction wave force f_d is expressed by

$$f_d = i2\pi\rho g R_P \sum_{p=1}^{N} \int_{R_{p-1}}^{R_p} \varphi_{7,0}^{I_p}(r, h_p - h) r \mathrm{d}r \tag{24}$$

Hydrodynamic coefficients μ and λ is expressed by

$$\mu + i\lambda/\omega = -2\rho\pi R_p \sum_{p=1}^{N} \int_{R_{p-1}}^{R_p} \varphi_{3,0}^{I_p}(r, h_p - h) r \mathrm{d}r \tag{25}$$

NUMERICAL RESULTS AND DISCUSSION

The wave energy convergence ability of oscillating body WEC is usually determined by physical parameter of PTO damping coefficients. In this section, the case of a inverted cone with angle α=90° and high t=10m is considered as a kind of vertical axisymmetric WEC. Linear as well as quadratic damping coefficients of PTO c have been examined based upon the optimized stiffness coefficient of PTO k according to resonance system.

$$k = \omega^2(m + \mu) - b \tag{26}$$

Power due to the linear PTO effect is depicted in Fig.9 for period T=5, 8, 10 and 12s, respectively. As shown in Fig.9, the power for higher periods is larger than that for lower periods. For different period T, there is a peak with varying linear damping coefficients of PTO c. In fact the peak position is

$$c = \lambda \tag{27}$$

It is not a surprise, due to it is the optimized damping coefficients of PTO c in order to satisfy the function $\partial_c P$=0.

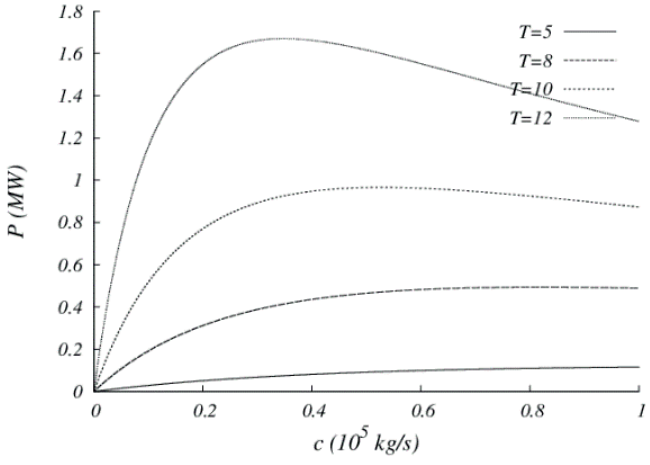

Fig.9. Power due to the linear PTO effect

Power due to the quadratic PTO effect depicted in Fig.10 for period T=5, 8, 10 and 12s, respectively.

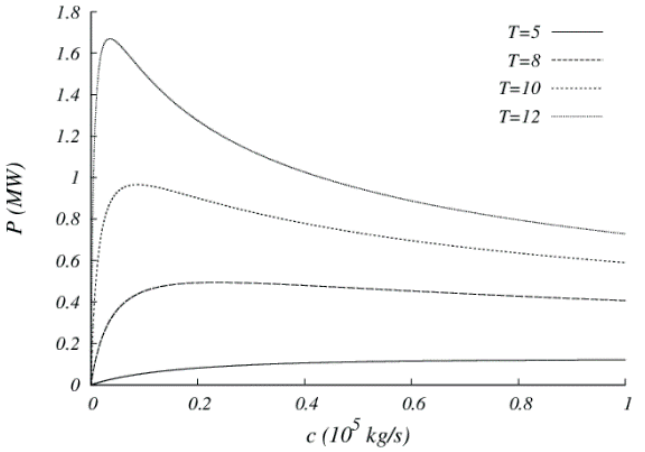

Fig.10. Power due to the quadratic PTO effect

Similar with power due to the linear PTO effect, the power for higher period is more than that for lower period and for different period T, there is a peak with varying linear damping coefficients of PTO c. However, the peak position is not as the linear PTO effect nearly the same with different period T and smaller than that for linear PTO effect. Fig.11 and Fig.12 shows the comparative results for power due to the linear and quadratic PTO effect at the higher period T=12 and the lower period T=5. Several important features can be observed in the Figs.

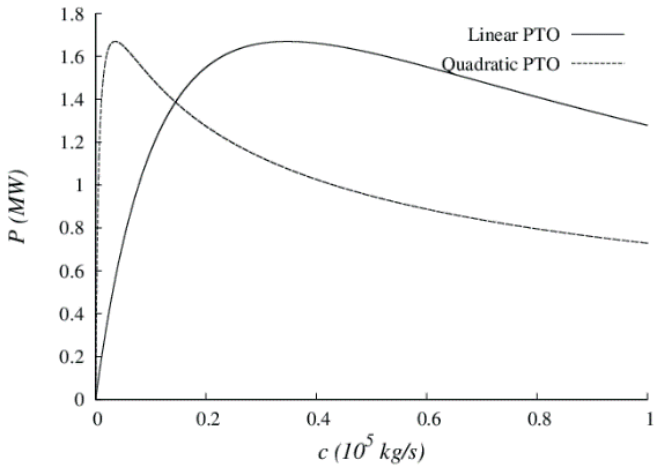

Fig.11 Power due to the linear and quadratic PTO effect at T=12

First, at the higher period T=12, it can be seen that the maximum power $P \approx 1.6(MW)$ is nearly the same but the peak position for quadratic PTO $c \approx 0.08(10^5\ kg/s)$ is smaller than that for linear PTO $c \approx 0.25(10^5\ kg/s)$, in other words, quadratic PTO effect can reach the peak before the linear PTO effect.

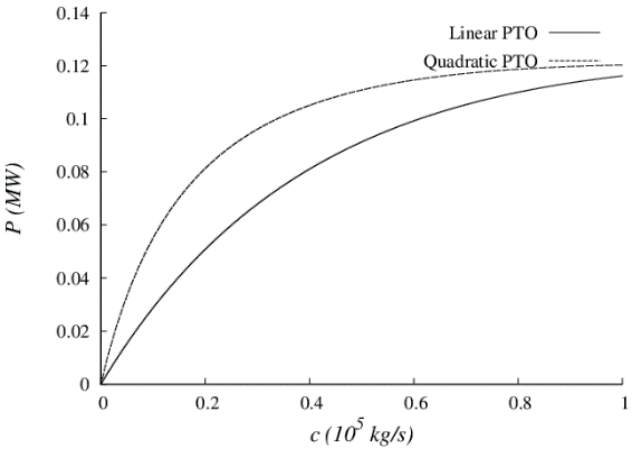

Fig.12. Power due to the linear and quadratic PTO effect at T=5

Second, also at higher period, there is a critical position $c \approx 0.18(10^5$ *kg/s*). At that position, power due to quadratic PTO is equal to power due to linear PTO. Before the critical position, the power due to quadratic PTO is higher, on the contrary, the power due to linear PTO is higher. Third, at the lower period *T*=5, power due to the quadratic PTO is always higher than power due to the linear PTO.

CONCLUSIONS

In this investigation, the linear and quadratic PTO effect have been applied in converting wave power into useful energy on the analytical method which is based on the series expansion of eigenfunctions. From the investigation, the following conclusions can be drawn:

(1). For linear PTO effect, the optimized linear damping coefficients of PTO *c* is obtained by the formulae and confirmed by the numerical results.

(2). For quadratic PTO effect, the optimized qudratic damping coefficients of PTO *c* is found by the numerical results.

(3). The comparisons have been made between the linear and quadratic PTO effect. At higher period, power due to quadratic PTO effect can reach the peak before the linear PTO effect. At the lower period, power due to the quadratic PTO is always higher than the linear PTO.

ACKNOWLEDGEMENT

This research is financially supported by the National Natural Science Foundation of China (No.51509048 and No.51679044).

APPENDIX A

The expression for known function $Z_0(z)$ and $Z_n(z)$ are given

$$Z_0(z) = \cosh k_0 h \cosh k_0 (z+h) \big(2k_0 h + \sinh 2k_0 h \big)$$

$$Z_n(z) = \cos k_n h \cos k_n (z+h) \big(2k_n h + \sin 2k_n h \big)$$

The coefficients ε_ℓ in velocity potential of incident wave are given

$$\varepsilon_\ell = \begin{cases} 1/Z_0(z) & (\ell = 0) \\ 2i^\ell / Z_0(z) & (\ell \geq 1) \end{cases}$$

The known function P(·), Q(·)and Ω(·) in diffraction and radiation potential are given

$$P_0^\ell(r) = \begin{cases} \ln(r/R_1)/\ln(R_2/R_1) & (\ell = 0) \\ [\, r/R_1)^\ell - (R_1/r)^\ell \,]/[(R_2/R_1)^\ell - (R_1/R_2)^\ell \,] & (\ell \geq 1) \end{cases}$$

$$\widetilde{P}_0^\ell(r) = \begin{cases} \ln(R_2/r)/\ln(R_2/R_1) & (\ell = 0) \\ [\, R_2/r)^\ell - (r/R_2)^\ell \,]/[(R_2/R_1)^\ell - (R_1/R_2)^\ell \,] & (\ell \geq 1) \end{cases}$$

$$Q_n^\ell(r) = \mathrm{K}_1^{n\ell} \mathrm{I}_\ell(\lambda_n r) - \mathrm{I}_1^{n\ell} \mathrm{K}_\ell(\lambda_n r)$$

$$\widetilde{Q}_n^\ell(r) = \mathrm{I}_2^{n\ell} \mathrm{K}_\ell(\lambda_n r) - \mathrm{K}_2^{n\ell} \mathrm{I}_\ell(\lambda_n r)$$

In which $\lambda n = n\pi/(h-d)$ and the constants are

$$\left\{ \mathrm{K}_1^{n\ell}, \mathrm{I}_1^{n\ell}, \mathrm{K}_2^{n\ell}, \mathrm{I}_2^{n\ell} \right\} = \frac{\mathrm{K}_\ell(\lambda_n R_1)\ \mathrm{I}_\ell(\lambda_n R_1)\ \mathrm{K}_\ell(\lambda_n R_2)\ \mathrm{I}_\ell(\lambda_n R_2)}{\mathrm{K}_\ell(\lambda_n R_1)\mathrm{I}_\ell(\lambda_n R_2) - \mathrm{K}_\ell(\lambda_n R_2)\mathrm{I}_\ell(\lambda_n R_1)}$$

$$\Omega_{7,\ell}^{\mathrm{I}}(r,z) = \phi_{0,\ell}$$

$$\Omega_{7,\ell}^{\mathrm{II}_{(1,2)},\mathrm{III}_{(1,2)},\mathrm{IV},\mathrm{V},\mathrm{VI}}(r,z) = 0$$

$$\Omega_{3,\ell}^{\mathrm{I,IV}}(r,z) = 0$$

$$\Omega_{3,\ell}^{\mathrm{II}_{(1,2)},\mathrm{V}}(r,z) = (z\omega^2 + g)/\omega^2$$

$$\Omega_{3,\ell}^{\mathrm{III}_{(1,2)},\mathrm{VI}}(r,z) = [2(z+h)^2 - r^2]/4(h-d)$$

REFERNCE

1. Tanaka H. Sea Trial of a Heaving Body Wave Power Absorber. Transactions of the Japan Society of Mechanical Engineers B, 1984, 50:2325-2333.

2. Budal K, Falnes J, Iversen LC, Lillebekken PM, Oltedal G, Hals. The Norwegian wave-power buoy project . In: Berge H, editor. Proceedings of 2nd International Symposium on Wave Energy Utilization, Trondheim, Norway; 1982, p.323-344.

3. Prado M. Archimedes wave swing (AWS) . In: Cruz J, editor. Ocean Wave Energy. Berlin: Springer, 2008. p. 297–304.

4. Elwood D, Schacher A, Rhinefrank K, Prudell J, Yim S, Amon E. Numerical modelling and ocean testing of a direct-drive wave energy device utilizing a permanent magnet linear generator for power take-off . In: Proceedings of 28th International Conference on Ocean Offshore Arctic Engineering, ASME, Honolulu, Hawaii, 2009, No.OMAE2009-79146.

5. L. Cameron, R. Doherty. Design of the Next Generation of the Oyster Wave Energy Converter. 3th International Conference on Ocean Energy, Bilbao, 2010: 1-12.

6. Harnessing the Blue Energy [R/OL]. (2010-06) [2012-07-06]. http://www.aw-energy.com/concept.html.

7. F. Flocard, T.D. Finnigan. Experiment investigation of power capture from pitching point absorbers. Proceedings of the 8th European Wave and Tidal Energy Conference, Uppsala, Sweden, 2009: 400-409.

8. Mavrakos SA, Katsaounis GM, Apostolidis MS (2009) Effects of floaters' geometry on the performance characteristics of tightly moored wave energy converters. In Proceedings of the 28th International Conference on Ocean Offshore Arctic Engineering, ASME, Honolulu, Hawaii, Paper No. OMAE 2009-80133.

9. Mehdi Nazari, Hassan Ghassemi, Mahmoud Ghiasi, Mesbah Sayehbani (2013) Design of the point absorber wave energy converter for Assaluyeh Port. Iranica Journal of Energy & Environment, 4(2):130-135.

10. Thomas Soulard, Marco Alves, António Sarmento (2009) Force reacting principle applied to a heave point absorber wave energy converter. In: The Nineteenth International Offshore and Polar Engineering Conference, Osaka, Japan, 21-26 June.

11. Jamie Goggins, William Finnegan (2014) Shape optimization of floating wave energy converters for a specified wave energy spectrum. Renewable Energy, 71:208-220.

12. Chakrabarti S K, Cotter D C, Libby A R. Hydrodynamic coefficients of a harmonically oscillated tower. Applied Ocean Research, 1983, 5(4):226-233.

13. Taylor R E, Drake K R, Duncan P E. The dynamics of a flexible articulated column in waves. Engineering Structures, 1983, 5(3):181-198.

14. Ran Z, Kim M H. Responses of Articulated Loading Platform in Irregular Waves. Journal of Waterway Port Coastal & Ocean Engineering, 1995, 121(6):283-293.

15. Caska A J, Finnigan T D. Hydrodynamic characteristics of a cylindrical bottom-pivoted wave energy absorber. Ocean Engineering, 2008, 35(1):6-16.

16. Stansby P, Moreno E C, Stallard T, et al. Three-float broad-band resonant line absorber with surge for wave energy conversion. Renewable Energy, 2015, 78:132-140.

17. Evans, D. V. (1976). A theory for wave-power absorption by oscillating bodies. Journal of Fluid Mechanics, 77(1), 1-25. (Journal)

18. Falnes, J. (2002). Linear interaction including wave-energy extraction. Ocean waves and oscillating system. Cambridge University press. (Textbook)

19. Wanan Sheng and Anthony Lewis (2016). Power Takeoff Optimization for Maximizing Energy Conversion of Wave-Activated Bodies. IEEE Journal of Oceanic Engineering, 1-12. (Journal)

20. Price, A. A. E., Dent, C. J., and Wallace, A. R. (2009). On the capture width of wave energy converters. Applied Ocean Research, 31(4), 251-259. (Journal)

21. Fitzgerald, J., & Bergdahl, L. (2008). Including moorings in the assessment of a generic offshore wave energy converter: a frequency domain approach. Marine Structures, 21(1), 23-46. (Journal)

22. Liu Haibin, Liu zhenling. (2010). "Recycling Utilization Patterns of Coal Mining Waste in China." Resources,Reservation and recycling(12): 1331-1340.

23. Eriksson, M., Isberg, J., and Leijon, M. (2005). Hydrodynamic modelling of a direct drive wave energy converter. International Journal of Engineering Science, 43(s 17–18), 1377-1387. (Journal)

24. Sheng, W., & Lewis, A. (2016). Power takeoff optimization for maximizing energy conversion of wave-activated bodies. IEEE Journal of Oceanic Engineering, 1-12. (Journal)

25. Cui, H. R., Liu, F. X., Armentani E., (2016). Analysis and assessment of the value of carbon assets based on

monte-carlo simulation. Journal of Mechanical Engineering Research and Developments 39 (2): 555-564.

26. Garrett CJR (1971) Waves forces on a circular dock. Journal of Fluid Mechanics, 46:129-39.

CONTACT WITH THE AUTHORS

Hengxu Liu

College of Shipbuilding Engineering
Harbin Engineering University
Harbin 150001
China